JOURNAL OF AGRICULTURAL AND FOOD CHEMISTRY

Denaturation and Aggregation of Three α-Lactalbumin Preparations at Neutral pH

MATTHEW K. MCGUFFEY,† KEVIN L. EPTING,‡ ROBERT M. KELLY,‡ AND E. ALLEN FOEGEDING*,†

Department of Food Science, Southeast Dairy Foods Research Center, North Carolina State University, 236 Schaub Hall, Raleigh, North Carolina 27695-7624, and Department of Chemical Engineering, North Carolina State University, 113 Riddick Labs, Raleigh, North Carolina 27695-7905

The denaturation and aggregation of reagent-grade (Σα-La), ion-exchange chromatography purified (IEXα-La), and a commercial-grade (Cα-La) α-lactalbumin were studied with differential scanning calorimetry (DSC), polyacrylamide gel electrophoresis, and turbidity measurement. All three preparations had similar thermal denaturation temperatures with an average of 63.7 °C. Heating pure preparations of α-lactalbumin produced three non-native monomer species and three distinct dimer species. This phenomenon was not observed in Cα-La. Turbidity development at 95 °C ($\tau_{95°C}$) indicated that pure preparations rapidly aggregate at pH 7.0, and evidence suggests that hydrophobic interactions drove this phenomenon. The Cα-La required 4 times the phosphate or excess Ca^{2+} concentrations to develop a similar $\tau_{95°C}$ to the pure preparations and displayed a complex pH-dependent $\tau_{95°C}$ behavior. Turbidity development dramatically decreased when the heating temperature was below 95 °C. A mechanism is provided, and the interrelationship between specific electrostatic interactions and hydrophobic attraction, in relation to the formation of disulfide-bonded products, is discussed.

KEYWORDS: α-Lactalbumin; whey proteins; denaturation and aggregation

INTRODUCTION

The ability of whey protein manufacturers to isolate α-lactalbumin (α-La) and β-lactoglobulin (β-Lg) to a high degree of purity represents a tremendous opportunity to broaden their food applications (*1*). Human milk contains ∼30% α-La (as a percent of the total protein), and the human and bovine variants have similar nutritional qualities including equally high tryptophan and cysteine contents (*2*). Because α-La shows minimum aggregation after heating (*3*), it is an excellent candidate for utilization in nutritional beverages, such as infant formulas and nutritional supplements.

α-La is a globular, calcium metalloprotein with a molecular weight (M_w) of 14.2 kDa, 4 disulfide bonds, and no free thiol groups (*4*). The two lobes of the three-dimensional structure (*5*, *6*) can be partitioned electrostatically (*7*): (1) an acidic lobe rich in β-sheet structure that contains the Ca^{2+}-binding loop (residues 35−88) (*5*, *6*) with a calculated pI of 3.7 (including 10 Asp) and (2) a basic lobe rich in α-helical structure (residues 1−34 and 89−123) (*5*, *6*) with a calculated pI of 9.6 (including 9 Lys).

The competition between electrostatic stabilization and intermolecular hydrophobic aggregation in denatured forms of α-La has been studied by evaluation in different solvent environments (*8*−*10*). With no additional salt, aggregation proceeds very slowly, but it is dramatically enhanced with the addition of Na_2SO_4 (*9*), potassium phosphate (*11*), and NaCl (*9*, *10*). The aggregation rate follows normal Hofmeister series effects, where salts that increase the surface tension of water increase the hydrophobic aggregation rate (*9*). This attraction can be significantly mitigated with the addition glycerol, ethyleneglycol, or poly(ethylene glycol) (i.e., solvents that interact with hydrophobic clusters) (*8*).

α-La denatures at relatively low temperatures (∼64 °C) but does not rapidly aggregate because of its lack of free thiol groups (*12*). However, when held at temperatures ≥85 °C, α-La evolves free thiol groups (*13*, *14*) that form intermolecular disulfide-bonded aggregates (*15*−*17*). Of the disulfide bonds of α-La (C6−C120, C28−C111, C61−C77, and C73−C91) (*18*), the C6−C120 disulfide bond is considered "super-reactive" (to DTT at 25 °C) because of the geometric strain imposed by the native fold, the positive charge distribution in this region, and its surface exposure (*19*, *20*). At 85 °C, it drives initiation of thiol/disulfide interchange, and, subsequently, a neighboring thiol (C111) is the most reactive in forming intermolecular disulfide bonds (*21*). The high reactivity on the C-terminus chain may be a result of its known flexibility (*21*, *22*) and the enhanced reactivity of Cys thiols in the proximity of positive charge density (*23*). Also, it has been suggested that hydrophobic interactions facilitate intermolecular disulfide bond formation in the co-aggregation of α-La and β-Lg (*17*, *24*).

* To whom correspondence should be addressed. E-mail: allen_foegeding@ncsu.edu.
† Department of Food Science, Southeast Dairy Foods Research Center.
‡ Department of Chemical Engineering.

10.1021/jf048863p CCC: $30.25
Published on Web 03/11/2005

Table 1. Summary of Treatment Conditions Where the Ability of α-Lactalbumin to Aggregate at High Temperature Was Evaluated (Listed Chronologically)

study	heat treatment	protein (g L^{-1})	solvent	α-La source	β-Lg present[a]	aggregation observed	method used
Chaplin and Lyster, 1986	100 °C for 10 min	14	0.10 M sodium phosphate buffer at pH 7	affinity chromatography purified	no	yes	PAGE
Calvo et al., 1993	90 °C for 24 min	1.5	"milk ultrafiltrate" composition not given	Sigma	NA[b]	no	SEC
Dagleigh et al., 1997	75 °C for 10 min	100	0.02 M phosphate buffer at pH 7	ion-exchange chromatography purified	no	no	SEC
Gezimati et al., 1997	80 °C for 15 min	80	"WPC-like" composition not given	Sigma	NA	no	PAGE
Schokker et al., 2000	80 °C for "prolonged heating"	10	0.02 M imidazole, 0.05 M NaCl, and 0.003 M NaN_3 at pH 7	Sigma (calcium saturated)	NA	no	SEC
Havea et al., 2000	75 °C for 6 min	50	WPC permeate (0.4 M K^+ and Na^+ and 0.035 M Ca^{2+} at pH 6.8	Sigma (calcium saturated)	NA	yes	PAGE
Bertrand-Harb et al., 2002	65, 85 and 95 °C for 30 min	10	0.2 M sodium phosphate buffer at pH 7.5	ion-exchange chromatography purified	yes	yes (≥85 °C)	PAGE
Hong and Creamer, 2002	70–95 °C (every 5 °C) for 10 min	2.4	0.015 M phosphate buffer at pH 6.7 or 7.4	size-exclusion chromatography purified	no	yes (≥80 °C)	PAGE

[a] Is β-Lg visually present in the electrophoretograms or chromatograms of the α-La preparations? [b] Not applicable (NA); Sigma α-La has no β-Lg contamination.

Most studies have evaluated the co-aggregation of α-La with β-Lg rather than with α-La alone. The consensus is that mixtures of α-La and β-Lg have enhanced aggregation properties than either protein heated alone (*25*). Even low relative concentrations of β-Lg in α-La preparations considerably enhance thermal aggregation (*12*, *15*, *26*); essentially, aggregate size increases as the β-Lg content is increased in α-La preparations (*12*). Chaplin and Lyster (*16*) provided the only study that focused solely on the heat-induced aggregation of α-La, and their proposed mechanism has not been significantly altered by subsequent studies. When α-La is heated to 77 °C (the temperature causing a complete unfolding transition as analyzed by DSC) and then cooled, it is >90% reversible. However, when α-La is held at 95 °C for 14 min, only 40% renatures to the native state. Native polyacrylamide gel electrophoresis (PAGE) shows the aggregates as small oligomers (dimers, trimers, etc.). Chaplin and Lyster (*16*) propose that irreversibility was due to the fact that a fraction of disulfide bonds are broken during heating of α-La at high temperatures, producing free thiol groups that can catalyze intermolecular thiol/disulfide interchange reactions that result in the formation of soluble oligomers (*16*).

There is considerable variation among studies investigating heat stability of α-La. **Table 1** lists eight studies that have evaluated α-La aggregation and the corresponding conditions inducing this phenomenon. Of the studies that observed *no* aggregation (*12*, *24*, *27*, *28*), three of the four studies: (1) used Sigma α-La, (2) were done at temperatures ≤80 °C, and (3) used size-exclusion chromatography (SEC) for analysis. The only study utilizing "extreme" temperatures (90 °C) (*27*) was done at the lowest concentration (1.5 g L^{-1}) and was analyzed by SEC. The only study that detected aggregates at temperatures <80 °C (*29*) was done at the lowest pH with a high ionic strength. This indicates that multiple factors including the α-La source, purity, temperature, concentration, and solvent may influence the denaturation/aggregation behavior. This study evaluates the denaturation and aggregation of the three α-La preparations used in the studies summarized in **Table 1**: (1) ion-exchange chromatography purified α-La (IEXα-La), (2) a reagent-grade preparation Sigma α-La (Σα-La), and (3) a commercial α-La preparation (Cα-La). This study examines the denaturation profile of these preparations to determine the relationship, if any, to aggregation. Microsensitive DSC utilizes a much lower protein concentration and a much higher sample volume than traditional instruments and is sensitive to microwatt changes in heat. This allows a thermodynamically appropriate interpretation of the denaturation results. To provide some perspective to the existing literature methods, *in situ* turbidity measurements were used to characterize the solvent and temperature dependence of α-La aggregation.

MATERIALS AND METHODS

Materials. The commercial α-La was a gift from Davisco Foods International (Le Sueur, MN) and contained 91.7% protein on a wet basis ($N \times 6.14$) (*30*) based on micro-Kjeldahl nitrogen analysis. This preparation was analyzed by reverse-phase high-performance liquid chromatography (HPLC) to determine its composition as a weight percent of the total protein. The preparation contained 92.5, 2.8, 0.8, 1.1, 0.6, and 2.2% α-La, β-Lg, BSA, immunoglobulin, glycomacropeptide, and proteose peptone, respectively. The Ca^{2+} concentration represented only ∼20% saturation of the α-La. The Na^+ concentration was 4300 ppm; K^+ and Mg^{2+} were <100 ppm; and Zn^{2+} and Mn^{2+} were found to be <1 ppm. Two different lots of highly purified α-La (product number L-5385) were obtained from Sigma Chemical Company (St. Louis, MO). A Q-Separose Fast Flow ion-exchange resin was used to purify the aforementioned commercial α-La according to Livney et al. (*21*). All salts and chemicals used were USP- or electrophoresis-grade.

General Methods. *Protein Solution Preparation*. Protein powder was hydrated with ∼90% of the total deionized H_2O (>17 MΩ) required and stirred for 2 h at room temperature. The order of salt solution addition was 0.2 M $CaCl_2$, 0.2 M sodium phosphate buffer (a blend of mono- and dibasic solutions to yield the reaction pH), and 1 M NaCl. The pH of this solution was adjusted using 0.10 N HCl, and then the balance of water was added. The intrinsic Ca^{2+} and Na^+ composition of the commercial preparation was compensated for in the total added.

The protein concentrations for purified holo- and apo-α-La preparations were calculated from light absorbance at 280 nm using extinction coefficients of 2.01 (*31*) and 1.95 L g^{-1} cm^{-1} (*4*), respectively. For the commercial α-La, an effective extinction coefficient was calculated using the protein content of the powder and determined to be $\epsilon_{280} = 1.92$ L g^{-1} cm^{-1}.

Native and SDS−PAGE. Native PAGE was performed using precast, 4−20% gradient gels made with Tris-HCl buffer (Bio-Rad Labs, Hercules, CA). Samples were diluted 1:2 with Bio-Rad "native sample buffer". The reservoir buffer was 0.02 M Tris and 0.2 M glycine at pH 8.0. Sodium dodecyl sulfate (SDS)−PAGE was performed under similar conditions, except that the protein samples were mixed with 1% SDS prior to 1:1 dilution in the native sample buffer and 0.1% SDS was added to the reservoir buffer. Protein staining was performed with a Coomassie Stain Solution (Bio-Rad Labs) for 1 h and destained with 10% glacial acetic acid and 10% 2-propanol overnight. A M_w marker containing myosin (200 kDa), β-galactosidase (116 kDa), phosphyorylase b (97.4 kDa), bovine serum albumin (66.2 kDa), and ovalbumin (45 kDa) from Bio-Rad was used. The naming convention of Hong and Creamer (*17*) was used to describe the products of heating α-La including nativelike and non-native monomers and SDS dimers.

DSC. The thermal denaturation of α-La was monitored using a Nano-Cal Model 5100 differential scanning calorimeter (Nano-DSC) (Calorimetry Sciences Corp., Provo, UT) using a scan rate of 1 °C min^{-1}. All solutions were thoroughly degassed prior to loading the instrument, and the cells were pressurized to ∼2 atm to prevent the formation of gas bubbles during heating. Samples of α-La (2.5 mg mL^{-1}) were dialyzed at 4 °C overnight against 1 L of 10 mM sodium phosphate

buffer (pH 7.0). The dialysis buffer was used to generate the baseline scan for analysis. A typical experiment consisted of a buffer/buffer scan set followed by a buffer/protein scan set (a set consists of 2 heating and cooling cycles from 25 to 95 °C).

The heat capacity data of the buffer and protein scans were analyzed using the CpCalc 2.0 software provided by the instrument manufacturer. The buffer scan (i.e., baseline) was subtracted from the protein scan, and the molar heat capacity was calculated using a molecular weight of 14.2 kDa for the α-La and a partial specific volume of 0.709 (*32*). A polynomial equation was used to fit the pretransition baseline to the post-transition baseline, and the area under this curve was used to calculate the calorimetric enthalpy (ΔH). The percent reversibility was calculated as the ratio of ΔH from the second heating scan to the first ($\Delta H_2/\Delta H_1 \times 100$). These data represent the average of three replications.

In Situ Turbidity Experiments. The time-dependent optical density development was monitored at 400 nm using a Shimadzu 160U spectrophotometer equipped with a jacketed cuvette holder attached to a recirculating water bath. For experiments at 95 °C, the water temperature initially was set to 100 °C to improve heat transfer and reduce the sample temperature lag. As the sample temperature approached 95 °C (~5 min), the water bath temperature was reduced to maintain a 95 °C sample temperature. For the 75 and 85 °C experiments, the temperature was initially set at 10 °C higher and then reduced to maintain the desired temperature. The sample temperature was monitored with a thermocouple every 2−3 min during the early stages of heating and every 10 min after it stabilized. The temperature accuracy was typically ±0.5 °C. At the end of the heating period, the protein solutions were rapidly cooled in water and the optical density (OD) was remeasured to assess the reversibility of aggregate formation. Visible concentration of aggregates at the bottom of the cuvette was only observed when heating pure preparations.

The OD values from the spectrophotometer were converted to turbidity (τ) values by the relationship ($\tau = 2.303 \times \mathrm{OD}/l$), where l represents the 1 cm path length (*33*). The reversibility was calculated as $(\tau_{95°C} - \tau_{25°C})/\tau_{95°C} \times 100$. The data represent the average of three replications for IEXα-La and Cα-La and two replications for Σα-La.

Statistical Analysis. The denaturation data was analyzed for statistical significance ($p < 0.05$) by analyzing through one-way ANOVA using the Microsoft Excel statistical package (Microsoft, Redmond, WA). The turbidity data were primarily analyzed for differences in trends, with error bars provided as indicators of variance.

RESULTS AND DISCUSSION

Purity of α-La Preparations. Figure 1A (lanes 2, 4, and 6) demonstrates the purity of the three preparations utilized in this study. The lanes were overloaded (40 μg of total protein) to visualize minor impurities. In the Cα-La (lane 6), the two higher mobility bands were the two variants of *β*-Lg, with *β*-Lg B being present at much higher concentrations. On the basis of the molecular mobility published by Kinghorn et al. (*34*), the two lower mobility bands appeared to be glycosylated α-La and either a α-La or α-La/*β*-Lg covalent dimer. Glycosylated α-La represented about 7% of the total as determined by deglycosylation by peptide *N*-glycosidase F and protein band quantitation by laser densitometry (data not shown). The presence of a dimer band in unheated Cα-La suggests that the rigors of the commercial process (pasteurization and spray drying) caused some aggregation. The Cα-La was used as the α-La source for IEX purification to provide a context in comparing results from the Σα-La and Cα-La preparations. Σα-La (lane 2) and IEXα-La (lane 4) demonstrated a similar high degree of purity with faint bands visible in the SDS−PAGE patterns corresponding to *β*-Lg and dimeric α-La.

Denaturation Profiles of α-La Preparations. Figure 2 shows the DSC denaturation profiles for Σα-La and IEXα-La. The dashed line represents the polynomial baseline fit with the area under the curve representing the calorimetric enthalpy (ΔH) and the peak of the curve representing the denaturation temperature (T_d). The only observation not consistent with previous work was a second peak observed in Σα-La with a T_d of ~85 °C that was not present in the IEXα-La. This is not

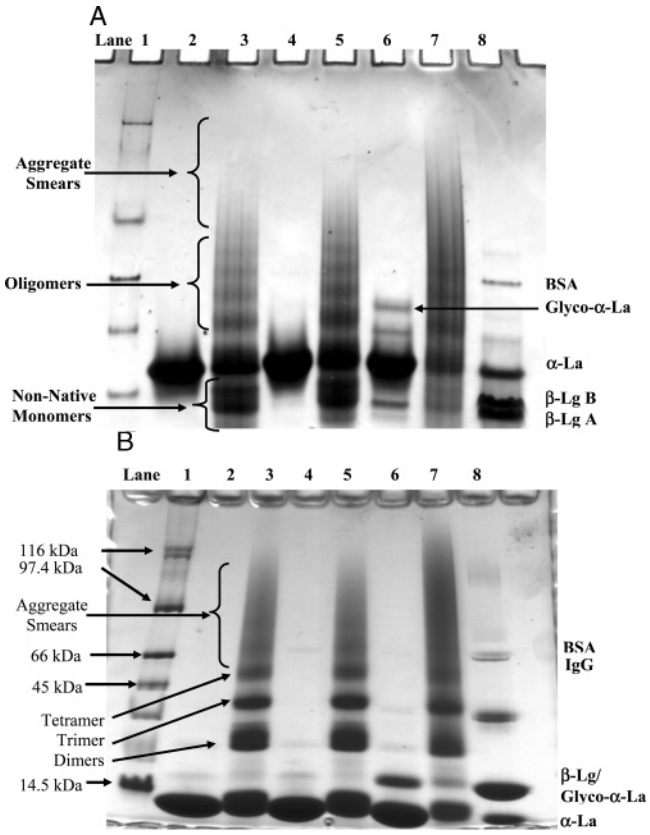

Figure 1. Native PAGE (A) and SDS PAGE (B) of the three preparations of native (even numbered lanes) and heated (odd numbered lanes) α-La (all containing 40 μg of total protein). Sigma and IEXα-La were heated for 30 min, and Cα-La was heated for 1 h at 95 °C. Lane 1 is the M_W marker; lanes 2 and 3 are Sigma α-La; lanes 4 and 5 are α-La isolated by ion-exchange chromatography; lanes 6 and 7 are commercial α-La; and lane 8 is the whey protein standard (30 μg of total protein). The heated solutions were obtained at the end of the heating periods from **Figure 4**.

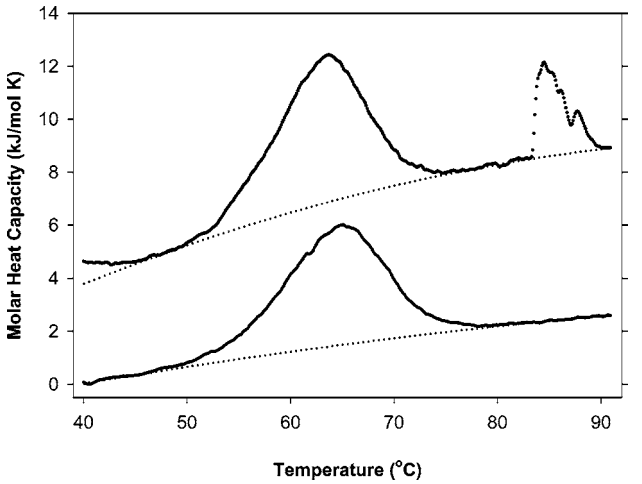

Figure 2. Two curves from the analysis of Sigma (top curve) and IEX (bottom curve) α-La by microsensitive differential scanning calorimetry. Solutions (~2.5 mg/mL) were heated at 1 °C/min in a 10 mM sodium phosphate buffer (pH 7), and the baseline was fit with a polynomial equation using software Calorimetry Sciences Corp., Provo, UT.

Table 2. Denaturation Parameters of Commercial, Ion-Exchange Chromatography Purified, and Sigma Holo-α-lactalbumin Preparations as Measured by Microsensitive Differential Scanning Calorimetry[a]

preparation	T_m (°C)	ΔH (kJ mol^{-1})	percent reversibility
commercial	63.1 ± 0.5 a	309 ± 2.0 b	34 ± 3.6 d
IEX	64.0 ± 1.4 a	261 ± 1.2 c	24 ± 1.7 e
Sigma	63.9 ± 0.3 a	286 ± 5.3 b,c	37 ± 0.6 d

[a] Values represent the mean ± standard deviation ($n = 3$). Values within a column with different letters are significantly different ($p < 0.05$).

seen when α-La is heated in Tris at pH 8.0 (*32*) and was not present on the second heating scan. Only the first peak was used to calculate the denaturation parameters described in **Table 2**. There was little difference in T_d between all three preparations (~63−64 °C). These values are consistent with studies using "microsensitive" DSC that found T_d values of 64.1 °C (*32*) and 64.2 °C (*35*) using 1 °C min^{-1} scan rates and similar concentrations. Previous investigations found a wider range of values including ~60 °C (*36*, *37*), 65 °C (*16*, *38*), and 70 °C (*39*). This variation arises from the use of widely varying solvent conditions, but more importantly, they use exceedingly higher protein concentrations (up to 200 mg mL^{-1}) to compensate for lack of instrumental sensitivity. Also, much higher scan rates were used (2.5−20 °C min^{-1}) and extrapolated down to 0 °C min^{-1}.

Table 2 shows the ΔH values obtained for the three preparations. Of the pure preparations, Σα-La (286 kJ/mol) required ~25 kJ/mol more energy to denature than IEXα-La (261 kJ/mol). The Cα-La required the most energy to denature (309 kJ/mol). The differences in ΔH for the purified preparations may represent a difference in their preparation procedures. The Σα-La was freeze-dried in the holo form, whereas IEXα-La was freeze-dried in the apo form and Ca^{2+} was added to the hydrated protein. The ΔH values for Σα-La and IEXα-La were consistent with previous determinations using microsensitive DSC: 264 kJ/mol (*32*) and 276 ± 9 kJ/mol (*40*).

The ability of α-La to undergo reversible denaturation transitions through multiple heat/cool cycles makes it unique among whey proteins (*38*, *41*). **Table 2** shows the similar percent reversibility values for Σα-La and Cα-La (~35%) with the slightly lower value obtained for IEX α-La (24%). The DSC automatically held the sample at the programmed terminal temperature (i.e., 95 °C) for 10 min before the cooling cycle to allow for system equilibration. These values are in reasonable agreement with the findings of Chaplin and Lyster (*16*),who found 40% reversibility when α-La is heated and held at 95 °C for 15 min before rescanning (10 °C min^{-1}; 1.6 mg mL^{-1}). When Σα-La was only heated to 90 °C, it was 72% reversible (data not shown), indicating that irreversible denaturation occurs much more rapidly at >90 °C. The apoprotein demonstrated an endothermic transition at 38 °C with no endothermic transition on the second scan (data not shown).

There are several examples in the literature where α-La displays very high reversibility including 80−90% (62 mg/mL; T_{max} = 110 °C at 10 °C/min) (*38*), >90% (~90 mg/mL; T_{max} = 95 °C at 21.4 °C/min) (*41*), and 100% through 4 heating cycles (200 mg/mL; T_{max} = 100 °C at 5 °C/min) (*39*). It is interesting that increased percent reversibility values correlate with a higher protein concentration. Eggers and Valentine (*42*) have demonstrated that the thermal stability of α-La is dramatically enhanced, while it is entrapped in a silica matrix (as compared to a dilute solution). They found that, at 95 °C, α-La had not approached complete unfolding, and they estimated an increase in T_d of 25−32 °C based on circular dichroism data (*42*). This type of phenomenon cannot be discounted in explaining the high degrees of renaturation in the very "crowded" systems sometimes utilized to obtain DSC data.

Analysis of Heated Preparations by PAGE. Figure 1A shows the loss of the monomer and formation of non-native monomers of higher mobility when α-La preparations were heated and analyzed by native PAGE. The Cα-La had a greater loss of the nativelike monomer and formed no non-native monomers (lane 7), although it was heated for 60 min. The pure preparations (lanes 3 and 5) formed three bands of higher mobility (two intense bands and one faint band) that corresponded to the non-native monomer bands described in previous studies (*16*, *17*). Differences in migration on native PAGE are based on differences in both net charge and hydrodynamic size; therefore, either the size decreased or the proteins possess a higher net negative charge than the nativelike monomer. The two studies that observed these species proposed different mechanisms for their formation. Chaplin and Lyster (*16*) proposed that higher mobility is caused by partial deamidation of glutamine and asparagines residues (thus, increasing net negative charge) because of their observation that heating α-La at 100 °C evolves ammonia (*16*). Hong and Creamer (*17*) suggested that intramolecular disulfide bond shuffling increases negative charge exposure because of the loss of Ca^{2+}-binding ability and that the differences in mobility among non-native monomer species represents a difference in hydrodynamic size. However, they acknowledged the need for "further fruitful study...to resolve these issues" (*17*).

Both native and SDS−PAGE results resolved 5 distinguishable bands of lower mobility (lanes 3, 5, and 7 in parts **A** and **B** of **Figure 1**) that Chaplin and Lyster (*16*) identified as oligomers by native PAGE. In SDS−PAGE patterns, three of these bands had similar mobility corresponding to SDS-dimeric species (two intense bands and one faint band) as observed by Hong and Creamer (*17*). They implicated differences in disulfide bond specificity that resulted in differences in hydrodynamic size (*17*). In Cα-La (lane 7), the oligomer bands were much less intense and there was only one distinct dimer band.

The other studies did not demonstrate the aggregate smearing observed in these PAGE patterns; however, they used a stacking/resolving gel system that appeared to trap aggregates at the interface between gels. The addition of SDS without any reducing agent did not appear to alter aggregate mobility, indicating that they were covalently bound as has been demonstrated (*15*, *16*). The Cα-La preparation had more of a smearing effect and formed aggregates that extended to 200 kDa. The purified preparations (heated for 30 min) formed aggregates that extended near the 116-kDa marker.

Concentration Dependence of Turbidity Development. The data in **Figure 3** shows the turbidity of the three α-La preparations (5−60 g/L) heated at 95 °C for 30 min and then cooled to 23 ± 2 °C. All of the treatments were of equal ionic strength (μ), where the absence of $CaCl_2$ in the apo treatments was compensated for with NaCl. In the treatments containing no Ca^{2+} (the apo conformer), there was very little turbidity development (i.e., formation of large aggregates) over the entire concentration range studied. This phenomenon was similar between preparations, with turbidity only deviating at ≥50 g/L. Holo-α-La developed higher turbidity than apo-α-La at protein concentrations ≥10 g/L (**Figure 3**). To illustrate, at 20 g/L, the Ca^{2+} concentration is only 1.4 mM, yet this causes a 28-fold larger turbidity value than the apo treatment with the same ionic strength.

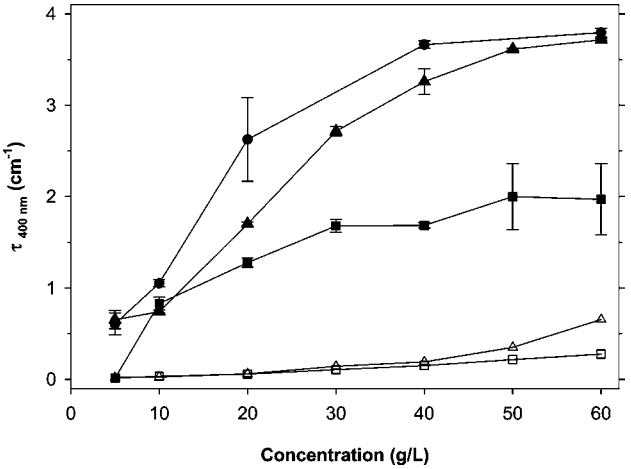

Figure 3. Concentration dependence of turbidity development after heating at 95 °C for 30 min for apo-α-lactalbumin (△ and □) and three holo-α-lactalbumin preparations (●, ▲, and ■): Sigma (●), IEX (▲ and △), and commercial (■ and □). Solutions contained 10 mM sodium phosphate buffered at pH 7 and 60 mM total Na (excess Na^+ was added as NaCl). Holo-α-La preparations contained a 1:1 molar ratio of Ca^{2+} to α-La. The 30 and 50 g L^{-1} treatments were not evaluated for Sigma α-La for cost considerations. Mean values (●, △, ▲, □, and ■) and standard deviations (error bars) of three replications are shown.

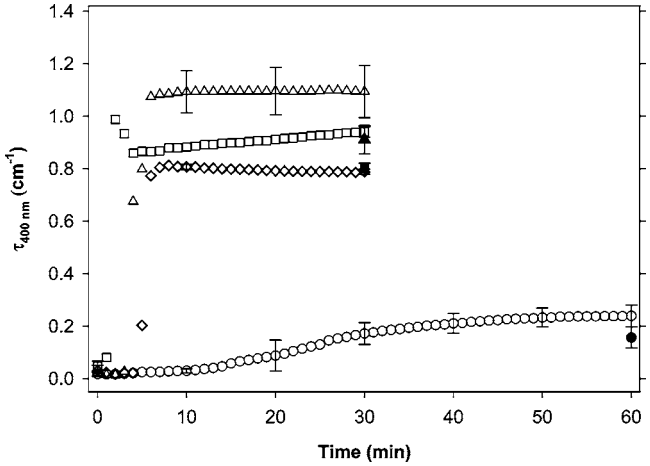

Figure 4. Turbidity development at 95 °C (○, □, and △) and its reversibility when cooled (●, ■, and ▲) of commercial (○ and ●), Sigma (□ and ■), and IEX (△ and ▲) holo-α-La and IEXα-La with 1 g/L β-Lg (◇). Solutions contained 10 g L^{-1} total protein and 10 mM sodium phosphate buffered at pH 7. Mean values (○, ●, □, ■, △, ▲, and ◇) and standard deviations (error bars) of three replications are shown.

The apo-α-La conformer has a much lower transition temperature ($T_d \sim 38$ °C) (*32*, *43*) and renaturation ability (*39*) than holo-α-La and has been referred to as more heat "labile" (*21*). It has also been found to be more "reactive" in the formation of non-native monomers and dimers (*17*). Also, the "slow reacting" disulfide bonds (C28−C111, C61−C77, and C73−C91) are reduced by DTT ∼40× (at 25 °C) faster in the apo conformer than the holo conformer (*19*). However, these cases of different reactivity did not lead to the formation of large aggregates (**Figure 3**), which is the most important consideration for beverage manufacturers.

There is more than one explanation to the increased aggregation of holo-α-La relative to apo-α-La. The presence of Ca^{2+} stabilizes the adjacent C61−C77 and C73−C91 disulfide bonds to thermal denaturation (*44*), and only the C61 forms disulfide-bonded aggregates when heated at 85 °C (*21*). Because denaturation probably leads to Ca^{2+} release (*35*), this cation either interacts favorably with the negative charge density on this lobe or bridges negative charges intermolecularly and facilitates hydrophobic interactions. This has been described for whey protein aggregation (*45*).

The Σα-La and IEXα-La preparations produced a significantly higher turbidity than Cα-La at concentrations >10 g/L (**Figure 3**). At concentrations ≥20 g/L, Σα-La formed white precipitates that settled out of the solution (these were resuspended prior to turbidity measurement). Only at 60 g/L did this occur for IEXα-La. One replication for all holo-α-La preparations was extensively dialyzed (a 10 mL sample against 10 L of deionized water with two exchanges). The dialyzed preparations were similar to undialyzed preparations, indicating that a dialyzable component (like residual salts) was not responsible for the differences in behavior. The remaining experiments were performed at 10 g/L to attempt to understand the phenomena that lead to aggregate stabilization or precipitation that occurred at a higher concentration.

Turbidity Evolution and Reversibility at 95 °C. Of the studies listed in **Table 1**, there were no measurements actually made at the temperature to which the protein was heated. For α-La, monitoring the turbidity development at 95 °C ($\tau_{95°C}$) proved to be valuable in understanding the pertinent interactions responsible for aggregate formation. **Figure 4** shows the $\tau_{95°C}$ development for the three preparations in the same electrostatic conditions (10 mM sodium phosphate at pH 7.0) as the DSC experiments. The highly purified Σ and IEX preparations formed very large aggregates that caused intense scattering as soon as the temperature exceeded T_d (∼3 min) and then reached a plateau throughout the remaining heating period. However, the $\tau_{95°C}$ of Cα-La did not begin its gradual increase until ∼15 min, and its plateau value was far lower than for purified α-La. Apparently, the minor protein constituents present in Cα-La or some other factor diminish rapid turbidity development. The presence of β-Lg in Cα-La would be the first logical explanation. However, when β-Lg was added to IEXα-La at levels mimicking the Cα-La, the $\tau_{95°C}$ trend was identical with a 28% decrease in its plateau turbidity value (**Figure 4**). There were two bands (not including the β-Lg variants) removed from Cα-La by the IEX chromatography purification process (**Figure 1A**) that caused it to behave similarly to Σα-La. They corresponded to glycosylated α-La and a dimer of α-La or α-La/β-Lg. Glycosylation by post-translational modification adds glucose to a solvent-exposed loop N45 (*46*). A covalent dimer could represent a charge alteration because of the loss of Ca^{2+}-binding ability with disulfide shuffling (*17*). When the glycosylated α-La and a dimer of α-La or α-La/β-Lg were removed, the system became unstable, resulting in intense turbidity development (**Figure 4**) and the formation of three separate non-native monomer bands (**Figure 1A**). Secondary-structure analysis on heated α-La reveals the formation of a new α helix that may represent a charge alteration (*47*). This may occur during the ingredient manufacturing process and provide thermal stability to Cα-La.

Figure 4 shows that the turbidity developed at 95 °C in α-La preparations was partially reversible upon cooling. The purified preparations had 15−20% reversibility, and the Cα-La was 35% reversible. Although the reversibility for Cα-La was large, it represented a slight decrease in a very low plateau turbidity value. The observed dissociation further suggests hydrophobic interactions as the logical explanation to the rapid turbidity development in denatured, purified α-La preparations. These interactions are favored at high temperatures and disfavored near room temperature (*48*).

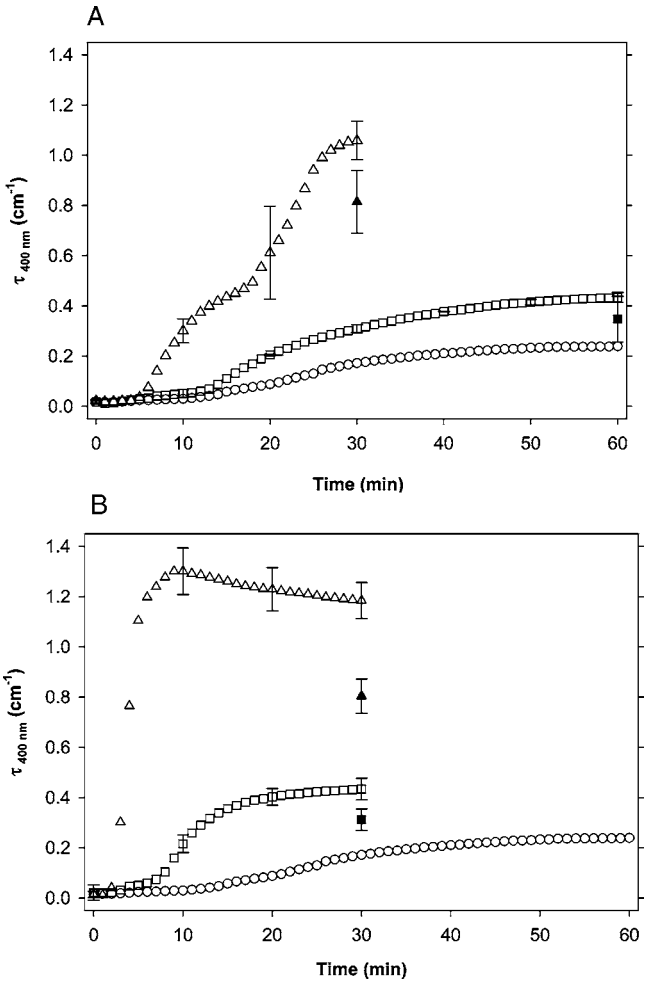

Figure 5. Effect of increasing monovalent (NaCl, A) and divalent (phosphate, B) salts on the turbidity development at 95 °C (□ and △) and its reversibility when cooled (■ and ▲) of commercial holo-α-lactalbumin (10 g L^{-1} total protein) at pH 7.0. The commercial α-La curve from **Figure 4** was represented in both A and B (○) to provide a visual reference. In A, NaCl was added to obtain a total Na^+ concentration of 30 mM (■ and □) and 60 mM (▲ and △). In B, sodium phosphate (buffered at pH 7.0) was added to obtain a 20 mM (■ and □) and 40 mM (▲ and △) phosphate concentration. The intrinsic Na^+ concentration contributed from the phosphate was 32 mM (20 mM) and 64 mM (40 mM). Mean values (○, □, ■, △, and ▲) and standard deviations (error bars) of three replications are shown.

Turbidity is not just a measure of aggregate size (i.e., M_w) but also a measure of shape, isotropy, and refractive properties (*49*). Purified preparations heated for 30 min had a 4× higher $\tau_{25°C}$ than Cα-La heated for 1 h (**Figure 4**), yet the aggregates of Cα-La had lower mobility when analyzed by PAGE (**Figure 1**). This indicates that the aggregates produced in the different preparations may have had different shapes. Because Cα-La demonstrated the greatest thermal stability, it was used for the remaining aggregation experiments.

Effect of the Solvent Environment on Turbidity Development in Cα-La. Figure 5A shows the increase in turbidity development with an increasing Na^+ concentration (added as NaCl with a constant phosphate concentration). The treatments with an ionic strength (μ) of 0.025 (16 mM Na^+) and 0.04 (30 mM Na^+) had similar $\tau_{95°C}$ trends with a slightly higher value with higher ionic strength. Further, increasing the μ to 0.07 (60 mM Na^+) resulted in a more abrupt $\tau_{95°C}$ increase. Interestingly, this treatment demonstrated a brief plateau in $\tau_{95°C}$ near 15 min

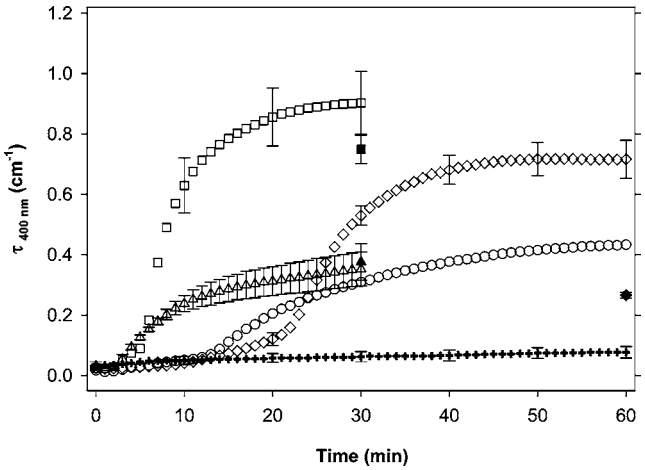

Figure 6. Effect of lowering the pH to 6.80 (◆ and ◇), 6.60 (+), and 6.00 (▲ and △) and adding a 2:1 molar ratio of Ca^{2+} to α-La at pH 7.0 (■ and □) on the turbidity development at 95 °C (◇, △, and □) and its reversibility when cooled (◆, ▲, and ■) for commercial holo-α-lactalbumin (10 g L^{-1} total protein). Solutions contained 10 mM sodium phosphate buffered at the given pH and ∼30 mM total Na^+. NaCl was used to compensate for the ionic strength (0.04 M) changes that occur with lowering the pH (on phosphate) or adding excess $CaCl_2$. The 30 mM Na curve from **Figure 5A** was represented (○) to provide a visual reference. Mean values (○, ◇, ◆, △, ▲, □, and ■) and standard deviations (error bars) of three replications are shown.

before rapidly increasing, suggesting that an intermediate was involved in the aggregation. Increasing the ionic strength from 0.04 to 0.07 decreased the reversibility from 31 to 16%.

Figure 5B shows the increase in $\tau_{95°C}$ when the phosphate concentration was increased from 10 to 40 mM. Doubling the phosphate concentration to 20 mM ($\mu = 0.045$) caused a rapid increase at ∼8 min that reached its plateau at 20 min and had 2× the plateau $\tau_{95°C}$ value over 10 mM phosphate. A further increase to 40 mM phosphate ($\mu = 0.09$) caused rapid $\tau_{95°C}$ development that was similar in magnitude to the pure preparations with only 10 mM phosphate. Increasing the ionic strength from 0.045 to 0.09 increased the reversibility from 16 to 34%.

Figure 6 shows the effects of decreasing the pH below 7.0 or adding excess Ca^{2+} (all treatments had equal ionic strength). Decreasing the pH to 6.8 increased the lag time but caused $\tau_{95°C}$ to develop to a higher terminal value than pH 7.0. However, when the pH was further lowered to 6.6, there was almost no $\tau_{95°C}$ development. A similar behavior was observed with a higher concentration of total Na^+ (data not shown). When the pH was lowered to pH 6.0, the $\tau_{95°C}$ development was immediate but it quickly reached a plateau value that was similar to pH 7.0. Decreasing the pH to 6.8 slightly increased its reversibility (44%), whereas the pH 6.0 treatment was not reversible at all (−6%).

The pH 6.6 results are opposite of what would be expected relative to the pI of α-La. The effect of pH may be related to two factors: (1) the concentration of $H_2PO_4^{-1}$ and HPO_4^{-2} ($pK_{a_2} = 6.86$) or (2) the decreased protein surface charge. The results suggest that decreasing the amount of HPO_4^{-2} from 5.8 mM at pH 7 to 3.5 mM at pH 6.6 (calculation based on the Henderson−Hasselback equation and not accounting for activity changes because of ionic strength) decreased aggregation more than the lowering if the protein surface charge. In other words, the potential for intermolecular cross-linking was more important in this pH range. However, further decreasing the pH to 6.0 enhanced $\tau_{95°C}$. This suggests that altering the protein surface charge enhances turbidity development. Another possibility is

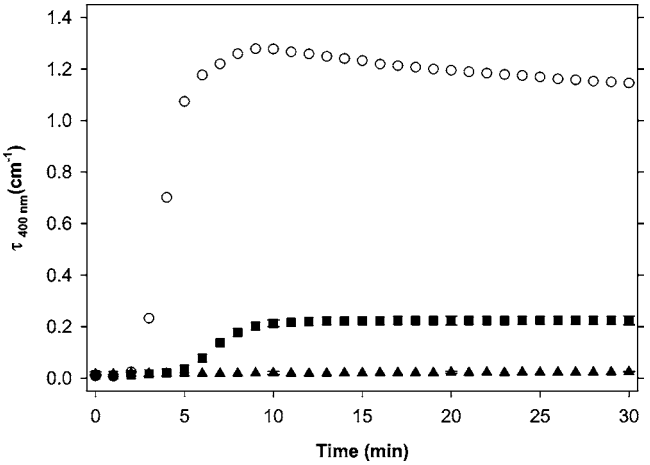

Figure 7. Temperature dependence of turbidity development for commercial α-La heated at 75 °C (▲) and 85 °C (■). Solutions contained 10 g L^{-1} total protein and 40 mM sodium phosphate buffered at pH 7 (contributing 64 mM total Na). The 40 mM sodium phosphate curve from **Figure 5B** was represented (○) to provide a visual reference. Mean values (▲, ■, and ○) and standard deviations (error bars) of three replications are shown.

the effect of phosphate on the α-La structure. Note that pH 6.6 is midway between the calculated pI values for the acidic loop (pI = 3.7) and basic lobe (pI = 9.6) (*5*, *6*). While no unambiguous conclusions can be made, given the prevalence of phosphate buffer as the buffer of choice for many aggregation studies (**Table 1**) and its use in protein beverages, these observations are important considerations for the stabilization of α-La.

There was a pronounced increase in $\tau_{95°C}$ in the presence of a 2:1 molar ratio of Ca^{2+}/α-La (**Figure 6**). The $\tau_{95°C}$ development was much more rapid than its 1:1 molar ratio counterpart and attained its plateau value around 25 min. The turbidity decreased slightly with cooling (17%). There are multiple roles that excess Ca^{2+} may be playing in this system to enhance interactions and aggregation. When α-La (∼3 mg/mL) is heated to 80 °C in the presence of excess Ca^{2+}, it retains some surface hydrophobicity that does not exist when heated with a 1:1 molar ratio (*50*). Mechanistically, the denaturation is converted from a simple two-step process ($N \rightarrow U + Ca^{2+}$) to a three-step process that possesses a Ca^{2+}-bound intermediate ($N \rightarrow I \rightarrow U + Ca^{2+}$) (*35*). Explained thermodynamically, adding excess Ca^{2+} reduces the highly positive entropy of Ca^{2+} mixing into the bulk solution that exists when a 1:1 molar ratio of Ca^{2+}/α-La is heated and loses its bound Ca^{2+} (*32*). Bovine α-La has a second, weaker Ca^{2+}-binding site involving H68 (*51*) that is adjacent to a hydrophobic cluster. A reduction in surface charge caused by this specific effect or a more general intermolecular ionic cross-linking might enhance rapid aggregation through hydrophobic interactions.

Temperature Dependence of Turbidity Development. There is a pronounced decrease in turbidity with a decreasing temperature (**Figure 7**). At 85 °C, there was a modest turbidity increase from 6 to 10 min with a plateau throughout the remaining heating time. At 75 °C, there was almost no turbidity development. Galani and Apenten (*52*) evaluated the contribution of hydrophobic interactions relative to disulfide bond formation in the aggregation of β-Lg (in WPI at pH 6.8) from 80 to 120 °C. The rate constant for hydrophobically driven aggregation is much larger at 95 °C than other temperatures (*52*). The irreversible denaturation (i.e., aggregation) of α-La heated in milk demonstrates an Arrhenius temperature dependence with a break at 80 °C (*53*, *54*). These studies demonstrating enhanced aggregation at temperatures >80 °C are consistent with the data seen in **Figure 7** and helps to explain the findings in **Table 1**, where most of the studies found no aggregation when heating at ≤80 °C.

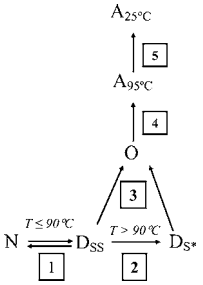

Figure 8. Mechanism for the heat-induced aggregation for both a pure and commercial source of holo-α-lactalbumin. N represents the native molecule; D_{ss} represents the denatured disulfide-intact monomer; D_{S*} represents a monomer with a reactive thiol; O represents an oligomer (dimer or trimer); $A_{95°C}$ represents large aggregates formed at 95 °C; and $A_{25°C}$ represents the dissociated aggregates at ambient temperature.

General Discussion. DSC has been used as a primary tool for measuring protein denaturation, and often, these results are extended to describe the "thermostability" of a protein. Ruegg et al. (*38*) stated that, "thermostability...should be interpreted in terms of renaturation and not of high temperatures of denaturation." However, this parameter does not evaluate the ability of the irreversibly denatured protein fraction to aggregate and become insoluble. In this study, Cα-La and Σα-La had similar abilities to renature but pronounced differences in turbidity development that lead to protein precipitation of Σα-La at ≥20 g/L. Furthermore, the most stable protein to aggregation, apo-α-La, had the lowest T_d and did not renature at all when heated and cooled under identical conditions. There was one denaturation parameter that was consistent with turbidity data. The increasing ΔH values for the three preparations (**Table 2**) corresponded to a decreasing extent of aggregation (**Figure 4**) in the same solvent conditions. Because protein aggregation is exothermic (*55*), this indicated that intermolecular interactions may have still been present at 2.5 g/L.

Figure 8 describes the mechanism for the heat-induced aggregation of α-La in 10 mM sodium phosphate (**Figures 1** and **4**). Steps 1−3 were proposed by Hong and Creamer (*17*), where steps 1 and 3 were based on the mechanism of Chaplin and Lyster (*16*). The mechanism was expanded with step 4 to represent the observations at 95 °C (**Figure 4**) and step 5 to represent the aggregate dissociation with cooling. When heated above T_d, α-La denatures and releases Ca^{2+} but does not rapidly undergo irreversible denaturation reactions at ≤90 °C and renatures when cooled (step 1). When held at >90 °C, pure α-La irreversibly denatures through intramolecular disulfide bond shuffling (step 2), forming three dominant non-native monomer species (**Figure 1A**) (*17*). In step 3, these species would have a free thiol group available to catalyze thiol/disulfide interchange and form the three dominant SDS-dimeric bands (**Figure 1B**) and larger oligomers. In Cα-La, irreversible denaturation proceeds directly through intermolecular thiol/disulfide interchange (step 3). Step 4 represents the formation of larger aggregate smears (parts **A** and **B** of **Figure 1**) that partially dissociate with cooling (step 5; **Figures 4**−**6**).

Denatured forms of α-La are referred to as molten-globule states, and an abundance of literature exists describing the forces responsible for its folding/unfolding in various conditions (for

a review, see refs *56* and *57*). The role that divalent phosphate played at high temperatures in facilitating hydrophobic interactions in molten-globule monomers (**Figure 4**) suggests the involvement of the basic lobe of the molecule. This lobe possesses the two most reactive thiol groups (C111 and C120) at 85 °C (*21*) and a hydrophobic cluster that is exposed upon Ca^{2+} release (*58*, *59*). This cluster contains the I27, M30, F31, and H32 residues from α-helix 2 and Q117 and W118 residues on the C terminus (*6*). Its folding/unfolding behavior is intricately involved with the C28−C111 disulfide bond (*60*−*62*), and it is much more stable to unfolding than the other hydrophobic cluster (*61*). Moreover, this cluster is shielded by a positive charge from L114 and probably one other residue (*63*). When L114 is replaced with an uncharged residue, the thermal stability to denaturation (i.e., T_d) increases by ∼11 °C (*22*), indicating that a positive charge density in this region destabilizes the cluster. The H32 residue may be the charge pair of the L114 because it has a pK_a' of ∼6.6 (*64*) and is adjacent to L114 in the native fold (*6*). This suggests that the ionization behavior of a specific residue like H32 might also be involved in the pH-dependent phenomena observed in this study. At pH 7.0, the −2 charged phosphate may stabilize this positive region and cause the exposed hydrophobic cluster to remain intact and facilitate rapid monomer association. This specific monomer−monomer contact may play a role in producing the specific intra- and intermolecular disulfide-bonded patterns seen in **Figure 1**. When α-La is heated to high temperatures at pH 6.6 (where phosphate has a −1 charge and some of the H32 is positively charged), the two positive charges might enhance reactivity of the neighboring C28−C111 disulfide bond (*23*), which would partially disorganize the native hydrophobic cluster and inhibit $\tau_{95°C}$ development (**Figure 6**). This is consistent with observations that C28 is unreactive and possibly "retracted inward" when heated at 85 °C (pH 6.0), despite extensive molecular unfolding and high reactivity from C111, its partner in the native molecule (*21*). This lack of C28 reactivity further indicates that this hydrophobic cluster remains intact and provides some protection to this part of the molecule, but more research is needed to verify this.

CONCLUSION

The aggregation of α-La was enhanced by the presence of calcium, a high degree of purity, excess ionic screening, and heating at 95 °C (relative to lower temperatures). Ionic screening was accentuated when α-La was heated in the presence of phosphate (−2 charge) or calcium (+2 charge). The turbidity decreased with cooling, suggesting a dissociation phenomenon. The formation of distinct disulfide-shuffled monomers and disulfide-bonded dimers may be related to specific hydrophobic interactions.

ACKNOWLEDGMENT

Paper FSR05-02 of the Journal Series of the Department of Food Science, North Carolina State University, Raleigh, NC 27695-7624. The use of trade names in this publication does not imply endorsement by the North Carolina Agricultural Research Service of the products named nor criticism of similar ones not mentioned.

LITERATURE CITED

(1) Smithers, G. W.; Ballard, F. J.; Copeland, A. D.; De Silva, K. J.; Dionysius, D. A.; Francis, G. L.; Goddard, C.; Grieve, P. A.; McIntosh, G. H.; Mitchell, I. R.; Pearce, R. J.; Regester, G. O. New opportunities from the isolation and utilization of whey proteins. *J. Dairy Sci.* **1996**, *79*, 1454−1459.

(2) Heine, W. E.; Klein, P. D.; Reeds, P. J. The importance of α-lactalbumin in infant nutrition. *J. Nutr.* **1991**, *121*, 277−283.

(3) Foegeding, E. A.; Davis, J. P.; Doucet, D.; McGuffey, M. K. Advances in modifying and understanding whey protein functionality. *Trends Food Sci. Technol.* 2002, *13*, 151−159.

(4) Swaisgood, H. E. Developments in dairy chemistry. In *Developments in Dairy Chemistry*; Fox, P. F., Ed.; Elsevier Applied Science Publishers: London, U.K., 1982; pp 132−147.

(5) Acharya, K. R.; Stuart, D. I.; Walker, N. P.; Lewis, M.; Phillips, D. C. Refined structure of babbon α-lactalbumin at 1.7 Å resolution. Comparison with c-type lysozyme. *J. Mol. Biol.* **1989**, *208*, 99−127.

(6) Chrysina, E. D.; Brew, K.; Acharya, K. R. Crystal structure of apo- and holo-bovine α-lactalbumin at 2.2-Å resolution reveal an effect of calcium on inter-lobe interactions. *J. Biol. Chem.* **2000**, *275*, 37021−37029.

(7) Vanhooren, A.; Vanhee, K.; Noyelle, K.; Majer, Z.; Joniau, M.; Hanssens, I. Structural basis for difference in heat capacity increments for Ca^{2+} binding to two α-lactalbumins. *Biophys. J.* **2002**, *82*, 407−417.

(8) Li, J.; Zhang, S.; Wang, C. C. Only the reduced conformer of α-lactalbumin is inducible to aggregation by protein aggregates. *J. Biochem.* **2001**, *129*, 821−826.

(9) Lindner, R. A.; Treweek, T. M.; Carver, J. A. The molecular chaperone α-crystallin is in kinetic competition with aggregation to stabilize a monomeric molten-globule form of α-lactalbumin. *Biochem. J.* **2001**, *354*, 79−87.

(10) Goers, J.; Permyakov, S. E.; Permyakov, E. A.; Uversky, V. N.; Fink, A. L. Conformational prerequisites for α-lactalbumin fibrillation. *Biochemistry* **2002**, *41*, 12546−12551.

(11) Li, H.; Errington, A. D.; Foegeding, E. A. Isostrength comparison of large-strain (fracture) rheological properties of egg white and whey protein gels. *J. Food Sci.* **1999**, *64*, 893−898.

(12) Dalgleish, D. G.; Senaratne, V.; Francois, S. Interactions between α-lactalbumin and *β*-lactoglobulin in the early stages of heat denaturation. *J. Agric. Food Chem.* **1997**, *45*, 3459−3464.

(13) Schnack, U.; Klostermeyer, H. Thermal decomposition of α-lactalbumin. 1. Destruction of cysteine residues. *Milchwissenschaft* **1980**, *35*, 206−208.

(14) Doi, H.; Tokuyama, T.; Kuo, F.-H.; Ibuki, F.; Kanamori, M. Heat-induced complex formation between *κ*-casein and α-lactalbumin. *Agr. Biol. Chem.* **1983**, *47*, 2817−2824.

(15) Bertrand-Harb, C.; Baday, A.; Dalgalarrondo, M.; Chobert, J. M.; Haertle, T. Thermal modifications of structure and co-denaturation of α-lactalbumin and *β*-lactoglobulin induce changes of solubility and susceptibility to proteases. *Nahr.-Food* **2002**, *46*, 283−289.

(16) Chaplin, L. C.; Lyster, R. L. J. Irreversible heat denaturation of bovine α-lactalbumin. *J. Dairy Sci.* **1986**, *53*, 249−258.

(17) Hong, Y. H.; Creamer, L. K. Changed protein structures of bovine *β*-lactoglobulin b and α-lactalbumin as a consequence of heat treatment. *Int. Dairy J.* **2002**, *12*, 345−359.

(18) Vanaman, T. C.; Brew, K.; Hill, R. L. Disulfide bonds of bovine α-lactalbumin. *J. Biol. Chem.* **1970**, *245*, 4583.

(19) Kuwajima, K.; Ikeguchi, M.; Sugawara, T.; Hiroka, Y.; Sugai, S. Kinetics of disulfide bond reduction in α-lactalbumin by dithiothreitol and molecular basis of superreactivity of the Cys6−Cys120 disulfide bond. *Biochemistry* **1990**, *29*, 8240−8249.

(20) Gohda, S.; Shimizu, A.; Ikeguchi, M.; Sugai, S. The superreactive disulfide bonds in α-lactalbumin and lysozyme. *J. Protein Chem.* **1995**, *14*, 731−737.

(21) Livney, Y. D.; Verespej, E.; Dalgleish, D. G. Steric effects governing disulfide bond interchange during thermal aggregation in solutions of *β*-lactoglobulin b and α-lactalbumin. *J. Agr. Food Chem.* **2003**, *51*, 8098−8106.

(22) Greene, L. H.; Grobler, J. A.; Malinovskii, V. A.; Tian, J.; Acharya, K. R.; Brew, K. Stability, activity, and flexibility in α-lactalbumin. *Protein Eng.* **1999**, *12*, 581−587.

(23) Bulaj, G.; Kortemme, T.; Goldenberg, D. P. Ionization−reactivity relationships for cysteine thiols in polypeptides. *Biochemistry* **1998**, *37*, 8965−8972.

(24) Gezimati, J.; Creamer, L. K.; Singh, H. Heat-induced interactions and gelation of mixtures of β-lactoglobulin and α-lactalbumin. *J. Agric. Food Chem.* **1997**, *45*, 1130−1136.
(25) de la Fuente, M. A.; Singh, H.; Hemar, Y. Recent advances in the characterization of heat-induced aggregates and intermediates of whey proteins. *Trends Food Sci. Technol.* **2002**, *13*, 262−274.
(26) Rattray, W.; Jelen, P. Thermal stability of skim milk whey protein solution blends. *Food Res. Int.* **1997**, *30*, 327−334.
(27) Calvo, S.; Leaver, J.; Banks, J. M. Influence of other whey proteins on the heat-induced aggregation of α-lactalbumin. *Int. Dairy J.* **1993**, *3*, 719−727.
(28) Schokker, E. P.; Singh, H.; Creamer, L. K. Heat-induced aggregation of β-lactoglobulin a and b with α-lactalbumin. *Int. Dairy J.* **2000**, *10*, 843−853.
(29) Havea, P.; Singh, H.; Creamer, L. K. Formation of new protein structures in heated mixtures of BSA and α-lactalbumin. *J. Agr. Food Chem.* **2000**, *48*, 1548−1556.
(30) Karman, A. H.; van Boekel, M. A. J. S. Evaluation of the Kjeldahl factor for conversion of the nitrogen content of milk and milk products to protein content. *Neth. Milk Dairy J.* **1986**, *40*, 315−336.
(31) Okazaki, A.; Ikura, T.; Nikaido, D.; Kuwajima, K. The chaperonin groel does not recognize apo-α-lactalbumin in the molten globule state. *Nat. Struct. Biol.* **1994**, *1*, 439−446.
(32) Hendrix, T.; Griko, Y. V.; Privalov, P. L. A calorimetric study of the influence of calcium on the stability of bovine α-lactalbumin. *Biophys. Chem.* **2000**, *84*, 27−34.
(33) Schorsch, C.; Jones, M. G.; Norton, I. T. Thermodynamic incompatibility and microstructure of milk protein/locust bean gum/sucrose systems. *Food Hydrocolloids* **1999**, *13*, 89−99.
(34) Kinghorn, N. M.; Norris, C. S.; Paterson, G. R.; Otter, D. E. Comparison of capillary electrophoresis with traditional methods to analyze bovine whey proteins. *J. Chromatogr., A* **1995**, *700*, 111−123.
(35) Vanderheeren, G.; Hanssens, I.; Meijberg, W.; VanAerschot, A. Thermodynamic characterization of the partially unfolded state of Ca^{2+}-loaded bovine α-lactalbumin: Evidence that partial unfolding can precede Ca^{2+} release. *Biochemistry* **1996**, *35*, 16753−16759.
(36) Bernal, V.; Jelen, P. Effect of calcium binding on thermal denaturation of bovine α-lactalbumin. *J. Dairy Sci.* 1984, *67*, 2452−2454.
(37) Relkin, P.; Eynard, L.; Launay, B. Thermodynamic parameters of β-lactoglobulin and α-lactalbumin. A DSC study of denaturation by heating. *Thermochim. Acta* **1992**, *204*, 111−121.
(38) Ruegg, M.; Moor, U.; Blanc, B. A calorimetric study of the thermal denaturation of whey proteins in simulated milk ultrafiltrate. *J. Dairy Res.* **1977**, *44*, 509−520.
(39) Boye, J. I.; Alli, I.; Ismail, A. A. Use of differential scanning calorimetry and infrared spectroscopy in the study of thermal and structural stability of α-lactalbumin. *J. Agric. Food Chem.* **1997**, *45*, 1116−1125.
(40) Pfeil, W. Thermodynamics of α-lactalbumin unfolding. *Biophys. Chem.* **1981**, *13*, 181−186.
(41) de Wit, J. N.; Klarenbeek, G. Effects of various heat treatments on structure and solubility of whey proteins. *J. Dairy Sci.* **1984**, *67*, 2701−2710.
(42) Eggers, D. K.; Valentine, J. S. Molecular confinement influences protein structure and enhances thermal protein stability. *Protein Sci.* **2001**, *10*, 250−261.
(43) Relkin, P.; Launay, B.; Eynard, L. Effect of sodium and calcium addition on thermal denaturation of apo-α-lactalbumin: A differential scanning calorimetric study. *J. Dairy Sci.* **1993**, *76*, 36−47.
(44) Chang, J.-Y.; Li, L. The structure of denatured α-lactalbumin elucidated by the technique of disulfide scrambling. *J. Biol. Chem.* **2001**, *276*, 9705−9712.
(45) Xiong, Y. L. Influence of pH and ionic environment on thermal aggregation of whey proteins. *J. Agric. Food Chem.* **1992**, *40*, 380−384.
(46) Slangen, C. J.; Visser, S. Use of mass spectrometry to rapidly characterize the heterogeneity of bovine α-lactalbumin. *J. Agric. Food Chem.* **1999**, *47*, 4549−4556.
(47) Fang, Y.; Dalgleish, D. G. The conformation of α-lactalbumin as a function of pH, heat treatment, and absorption at hydrophobic surfaces studied by FTIR. *Food Hydrocolloids* **1998**, *12*, 121−126.
(48) Dill, K. A. Dominant forces in protein folding. *Biochemistry* **1990**, *29*, 7133−7155.
(49) Cancellieri, A.; Frontali, C.; Gratton, E. Dispersion effect on turbidimetric size measurement. *Biopolymers* 1974, *13*, 735−743.
(50) Vanderheeren, G.; Hanssens, I. Thermal unfolding of bovine α-lactalbumin. *J. Biol. Chem.* **1994**, *269*, 7090−7094.
(51) Aramini, J. M.; Drakenberg, T.; Hiraoki, T.; Ke, Y.; Nitta, K.; Vogel, H. J. Ca-43 NMR-studies of calcium-binding lysozymes and α-lactalbumins. *Biochemistry* **1992**, *31*, 6761−6768.
(52) Galani, D.; Apenten, R. K. O. Heat-induced denaturation and aggregation of β-lactoglobulin: Kinetics of formation of hydrophobic and disulphide-linked aggregates. *Int. J. Food Sci. Technol.* **1999**, *34*, 467−476.
(53) Dannenberg, F.; Kessler, H.-G. Reaction kinetics of the denaturation of whey proteins in milk. *J. Food Sci.* **1988**, *53*, 258−263.
(54) Anema, S. G.; McKenna, A. B. Reaction kinetics of thermal denaturation of whey proteins in heated reconstituted whole milk. *J. Agric. Food Chem.* **1996**, *44*, 422−428.
(55) Marshall, W. E.; Zarins, Z. M. Exothermic transitions of glycinin determined by differential scanning calorimetry. *J. Agr. Food Chem.* **1989**, *37*, 869−873.
(56) Kuwajima, K. The molten globule state of α-lactalbumin. *FASEB J.* **1996**, *10*, 102−109.
(57) Permyakov, E. A.; Berliner, L. J. α-Lactalbumin: Structure and function. *FEBS Lett.* **2000**, *473*, 269−274.
(58) Lindahl, L.; Vogel, H. J. Metal-ion dependent hydrophobic interaction chromatography of α-lactalbumins. *Anal. Biochem.* **1984**, *140*, 394−402.
(59) Desmet, J.; Vancauwelaert, F. Calorimetric experiments of Mn^{2+}-binding to α-lactalbumin. *Biochim. Biophys. Acta* **1988**, *957*, 411−419.
(60) Peng, Z. Y.; Wu, L. C.; Kim, P. S. Local structural preferences in the α-lactalbumin molten globule. *Biochemistry* **1995**, *34*, 3248−3252.
(61) Wu, L. C.; Kim, P. S. A specific hydrophobic core in the α-lactalbumin molten globule. *J. Mol. Biol.* 1998, *280*, 175−182.
(62) Song, J. X.; Bai, P.; Luo, L.; Peng, Z. Y. Contribution of individual residues to formation of the native-like tertiary topology in the α-lactalbumin molten globule. *J. Mol. Biol.* **1998**, *280*, 167−174.
(63) Richardson, R.; Brew, K. Lactose synthase. An investigation of the interaction site of α-lactalbumin for galactosyltransferase by differential kinetic labeling. *J. Biol. Chem.* **1980**, *255*, 3377−3385.
(64) Bradbury, J. H.; Norton, R. S. Proton-magnetic-resonance spectroscopic study of histidine residues of bovine α-lactalbumin. *Eur. J. Biochem.* **1975**, *53*, 387−396.

Received for review July 9, 2004. Revised manuscript received January 25, 2005. Accepted February 9, 2005. Support from the North Carolina Agricultural Research Service, Dairy Management Incorporated, Southeast Dairy Foods Research Center and NSF Grant No. BES-0115734 is gratefully acknowledged.

JF048863P